Pergamon

PII: S0360-5442(96)00102-8

Energy Vol. 22, No. 4, pp. 437–447, 1997

0360-5442/97 $17.00 + 0.00

SILICA GEL WATER ADVANCED ADSORPTION REFRIGERATION CYCLE

BIDYUT B. SAHA, ATSUSHI AKISAWA and TAKAO KASHIWAGI†

Kashiwagi Laboratory, Department of Mechanical Systems Engineering, Tokyo University of Agriculture and Technology, 2-24-16 Naka-machi, Koganei-shi, Tokyo 184, Japan

(Received 29 May 1996)

Abstract—We present results of an analytic investigation on the influence of the thermal conductance of sorption elements (adsorber/desorber, evaporator and condenser) on the performance of a silica-gel–water advanced adsorption chiller, with consideration of the thermal capacitance ratio of the adsorbent and metal of the adsorber/desorber heat exchanger. The analysis was performed by using a cycle-simulation model developed by us and a coworker. The chiller is driven by exploiting waste heat at a temperature 50°C with a cooling source at 30°C for air-conditioning and refrigeration purposes. The results show that the cycle performance is strongly affected by the thermal capacitance and adsorber/desorber thermal conductance due to severe sensible heating/cooling requirements resulting from batched cycle operation. The model is somewhat sensitive to the thermal conductance of the evaporator. The thermal conductance of the condenser is the least sensitive parameter, as the adsorption behavior of the adsorbent/adsorbate pair at a fixed temperature is defined for desorption and condensation. © 1997 Elsevier Science Ltd. All rights reserved.

INTRODUCTION

The performance of an advanced, three-stage, silica-gel–water chiller utilizing low-grade waste heat between 60 and 40°C as the driving heat source with a cooling source at 30°C was investigated analytically by Saha et al.[1] The main innovative feature of the three-stage chiller is the ability to operate with a small regenerating temperature lift and it is therefore attractive as an energy saver. On the other hand, the use of fixed beds requires the adsorbent to be repeatedly switched between adsorption and desorption modes, which causes severe irreversible heat losses as the result of the batch-cycle operation.

In order to improve the cycle efficiency by reducing irreversibilities in batch-cycle operation, several advanced cycles have been proposed by various authors. Shelton et al[2] used a thermal wave cycle with adsorber/desorber heat recovery by which heat losses are reduced in fixed-bed cycles. Härkönen and Aittomäke[3] describe a ramp-wave cycle with parallel temperature ramps in the fluid and adsorbent bed. Meunier[4] and Douss and Meunier[5] analyzed the heat integration problem by introducing cascaded cycles from the same perspective.

In this paper, a model developed by Saha et al[1] is utilized. The cycles under study operate with $T_{des} = 50°C$ and $T_{ads} = 30°C$. The short cycle times adopted (the adsorption–desorption cycle time is 300s and the sensible heat exchange cycle time is 30s) require rapid and efficient sensible heat exchange between the adsorbers or desorbers and the external heat-transfer fluids (cold or hot water) for the cycle to work effectively. The adsorbent-to-metal heat-capacitance ratio and the adsorbent mass inside each adsorber or desorber heat exchanger are taken as the most important parameters for heat exchange and cycle performance.

THE WORKING PRINCIPLE OF THE CHILLER

The chiller consists of eight heat exchangers, namely, a condenser, an evaporator and three pairs of adsorber–desorber heat exchangers, plus eight refrigerant valves and one expansion valve, as shown in Fig. 1. Refrigerant valves 1, 3, 6, and 8 are open to allow refrigerant flow between heat exchangers; while the desorbers 1, 3 and 5 are heated by hot water, adsorbers 2, 4 and 6 are cooled by cooling water.

†Author for correspondence. Fax: 81-423-887012, e-mail: kasiwagi@cc.tuat.ac.jp

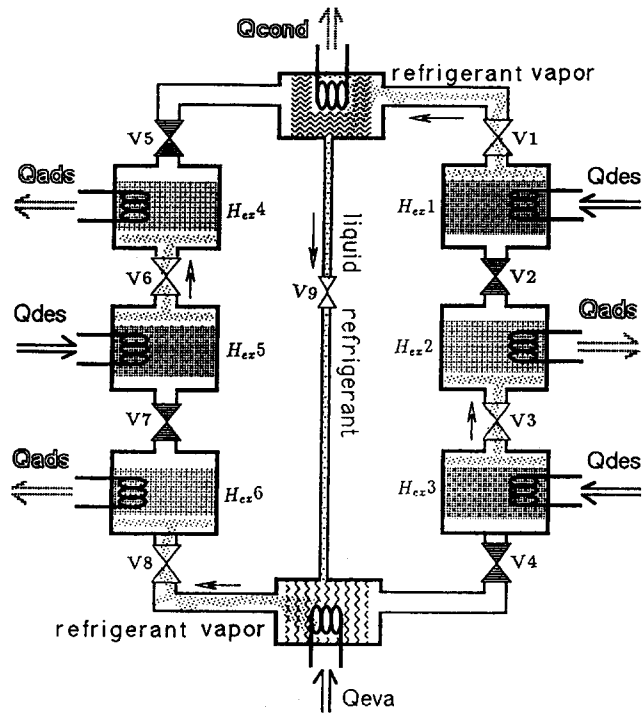

V = valve; H_{ex} = heat exchanger

Fig. 1. Schematic of the 3-stage adsorption chiller.

Refrigerant (water) is evaporated at the temperature T_{eva} with heat input Q_{eva} from the chilled water and is adsorbed by adsorber 6. The heat exchangers 2 and 4 adsorb refrigerant from desorbers 3 and 5, respectively. Desorbers are heated to the temperature T_{des} by the heat input Q_{des}. Desorber 1 is connected to the condenser, where the desorbed refrigerant vapor is condensed at the temperature T_{cond}; cooling water removes the condensation heat Q_{cond}. The resulting condensate flows back to the evaporator via valve 9 to complete the cycle.

On completion of the desorption–adsorption cycle of 300s, the flows of hot and cold water are redirected by switching all refrigerant valves so that desorbers 1, 3 and 5 operate in an adsorption mode and adsorbers 2, 4 and 6 change to desorption operation. This change is preceded by a sensible heat-exchange cycle of 30 s duration during which no adsorption or desorption occurs.

NUMERICAL SIMULATION

The influence of adsorbent mass and thermal conductance of the sorption elements on cooling capacity, power density, COP, and chiller efficiency (η = COP/Carnot COP) was investigated with a dynamic model.[1] The model has been validated by comparison with experimentally obtained heat balances for the heat-transfer-fluid temperatures (hot, cold and chilled) and flow rates. In the model, the following simplifying assumptions are made: (i) refrigerant mass flows between evaporator/adsorber, desorber/condenser and adsorber/desorber are equivalent, (ii) adsorption/desorption equilibrium is attained at all times; (iii) no adsorption/desorption occurs during sensible heat exchange process; (iv) all three adsorbers (or desorbers) operate at the same temperatures; (v) the dependences of specific heats on temperature and of adsorption heat on concentration are neglected; (vi) the effects of external heat losses and non-condensable gases are neglected.

Properties of moist silica gel

Adsorption equilibrium—We have utilized a modified Freundlich equation[1] to provide a concise analytical expression for the experimental data in the following form:

$$q^* = A(T_s) \times [P_s(T_w)/P_s(T_s)]^{B(T_s)}, \quad (1)$$

where

$$A(T_s) = A0 + A1 \times T_s + A2 \times T_s^2 + A3 \times T_s^3,$$
$$B(T_s) = B0 + B1 \times T_s + B2 \times T_s^2 + B3 \times T_s^3.$$

Here, q^* is the amount adsorbed at equilibrium at the pressure $P_s(T_w)$. The numerical values of $A0$–$A3$ and $B0$–$B3$ are determined by applying the least-squares method to the experimental data.

Adsorbtion rate—The adsorption rate is considered to be controlled by surface diffusion inside a particle. The surface diffusivity is[6]

$$D_s = D_{so} \times \exp[-E_a)/(RT)], \tag{2}$$

where D_{so}, E_a and R denote, respectively, the pre-exponential constant, activation energy for surface diffusion and real gas constant. The overall mass-transfer coefficient ($ksap$) for adsorption is

$$ksap = (15D_s)/(R_p^2), \tag{3}$$

and the adsorption rate is

$$dq/dt = ksap \times (q^* - q). \tag{4}$$

Mass and heat balances

The mass- and heat-balance equations for adsorption or desorption and evaporation or condensation are discussed elsewhere.[1,7]

COP and chiller efficiency η

The COP and chiller efficiency η are defined by the following equations:[1,8]

$$\mathrm{COP} = Q_{chill}/Q_{hot}, \tag{5}$$
$$Q_{chill} = C_{p\,chill} \times m_{chill} \times (T_{chill\,in} - T_{chill\,out}), \tag{6}$$
$$Q_{hot} = C_{p\,hot} \times m_{hot} \times (T_{hot\,in} - T_{hot\,out}), \tag{7}$$

and

$$\eta = \mathrm{COP}/\mathrm{COP}_{Carnot}, \tag{8}$$

where

$$\mathrm{COP}_{Carnot} = [(\overline{T}_{des} - \overline{T}_{cond})/\overline{T}_{des}] \times [\overline{T}_{eva}/(\overline{T}_{ads} - \overline{T}_{eva})] \tag{9}$$

with $\overline{T}_{des}$, $\overline{T}_{cond}$, $\overline{T}_{ads}$ and $\overline{T}_{eva}$ indicating, respectively, the average temperatures inside the desorber, condenser, adsorber, and evaporator during one cycle.

SIMULATION PROCEDURE

A numerical integration technique was used in solving Eqs. (1)–(4) along with the mass- and heat-balance.[1,7] Finite difference substitutions were made in the derivatives of the equations. In the numerical solution of the equations, successive substitutions of the newly calculated values were used, with the iterative loop repeating the calculations until the convergence test was satisfied. The calculations were made for a time interval of one second. The solution was taken to have converged when heat balances

for all heat exchangers coincided within 2%. The convergence factor was taken as 0.001 for all parameters. A flow diagram of the program is shown in Fig. 2.

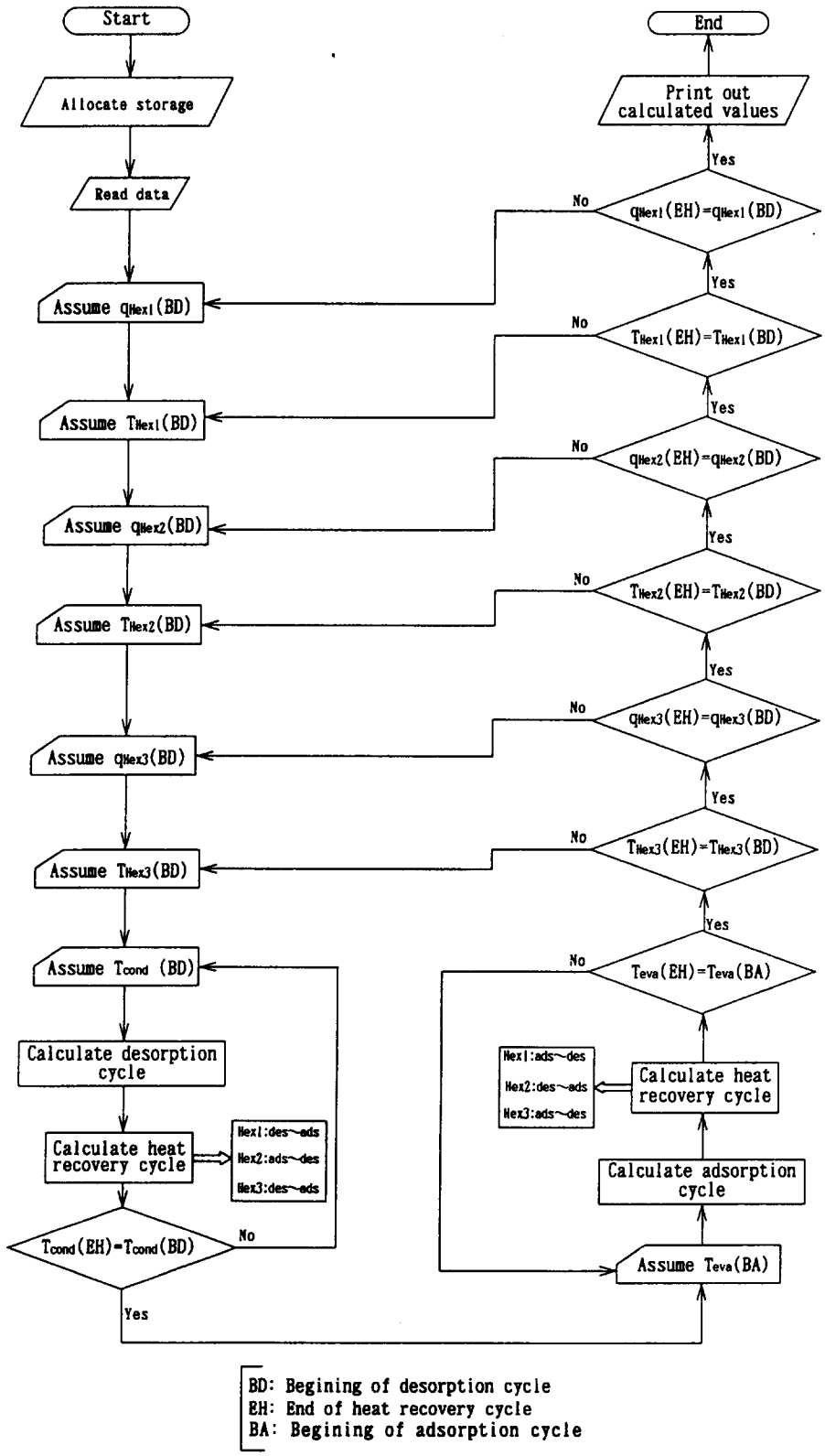

Fig. 2. Computer program — sequence of operations.

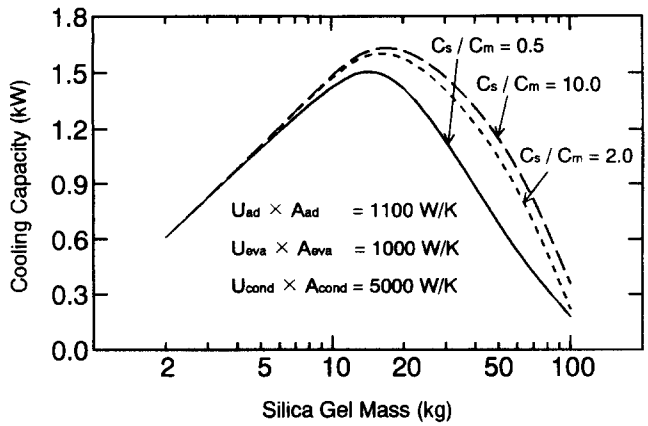

Fig. 3. (a) The effect of adsorbent mass on cooling capacity.

RESULTS AND DISCUSSION

In order to improve the system performance the sensitivity of the model is discussed in terms of the following parameters: (i) adsorbent mass in the adsorber/desorber heat exchanger; (ii) adsorbent-to-metal thermal capacitance ratio in the adsorber/desorber; (iii) adsorber/desorber thermal conductance; (iv) evaporator thermal conductance.

The thermal conductance of the condenser is omitted as it has very little effect on cooling capacity, power density, COP, and chiller efficiency η. The thermal conductance is determined by multiplying the heat-transfer coefficient (U) and the effective surface area (A) of the heat exchanger. The thermal conductance can be improved by increasing the heat-transfer coefficient with a change of material or by varying such external parameters as heat-transfer, fluid-flow rates, cycle times, etc. It may also be increased by an increase of the total surface area of the heat exchanger.

Silica-gel mass

Figure 3 (a)–(d) show results obtained for the effects of silica-gel mass on cooling capacity, power density, COP, and chiller efficiency η, respectively. Two regions appear in the graphs corresponding to distinct cycle-behavior patterns. The first region corresponds to relatively large adsorber/desorber heat exchangers (containing less than 12 kg of SiO_2). The results show a needed increase of SiO_2 mass to be effective in the first region, since the cooling capacity and chiller efficiency η increase substantially while the power density and COP decrease moderately as the adsorbent mass is increased. It should be noted that in the first region, the thermal conductances $U \times A$ of adsorber/desorber, evaporator and condenser become relatively high, particularly in the range below 10 kg of SiO_2, since the thermal conductance values for adsorber/desorber, evaporator and condenser are kept at the standard levels as shown in Table 1 throughout the entire range of the SiO_2 mass values.

The second region corresponds to relatively heavy heat exchangers, where increasing the adsorbent

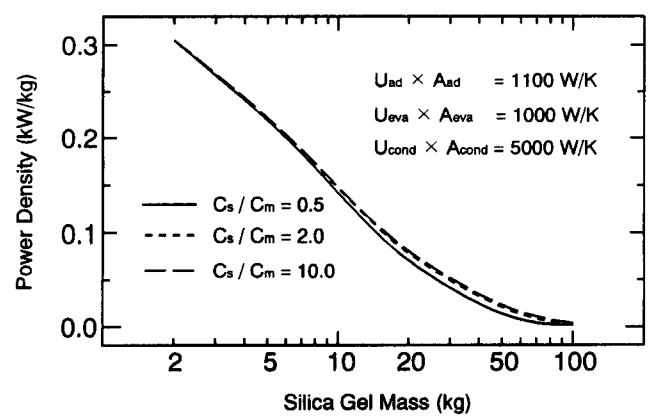

Fig. 3. (b) The effect of adsorbent mass on power density.

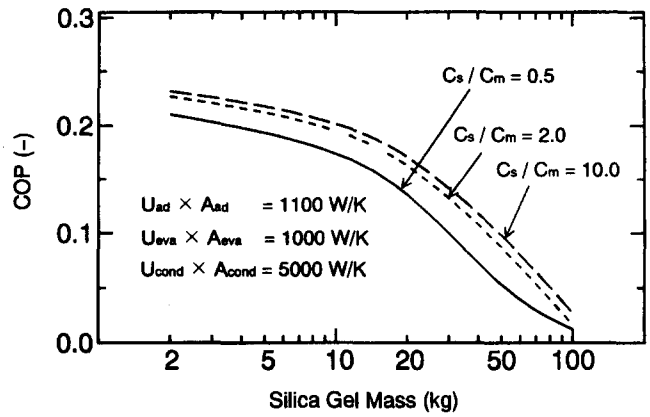

Fig. 3. (c) The effect of adsorbent mass on COP.

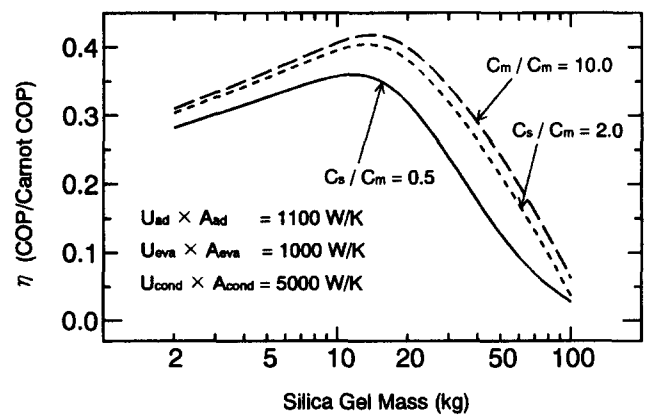

Fig. 3. (d) The effect of adsorbent mass on chiller efficiency η.

Table 1. Physical property values.

Values Adopted in Simulation		
Symbol	Value	Unit
C_{pAl}	905	J/kg × K
C_{pCu}	386	J/kg × K
C_{pchill}	4180	J/kg × K
C_{phot}	4180	J/kg × K
C_{ps}	924	J/kg × K
D_{so}	2.54×10^{-4}	m^2/s
E_a	4.2×10^4	J/mol
R_p	1.7×10^{-4}	m
$U_{ad} \times A_{Hex}$	1100.0	W/K
$U_{cond} \times A_{cond}$	5000.0	W/K
$U_{eva} \times A_{eva}$	1000.0	W/K
W_{cond}	3.84	kg
W_{eva}	2.4	kg
W_{fHex}	1.99	kg
W_{kHex}	2.49	kg

mass results in reducing the cooling capacity. This tendency is attributed mainly to the fact that the standard values employed for the thermal conductances of the adsorber/desorber, evaporator and condenser become relatively low when the adsorbent mass is increased beyond 30 kg of SiO_2 as in Fig. 3(a). As will be shown, the increased adsorber/desorber mass can only be cooled or heated effectively if the thermal conductances are increased.

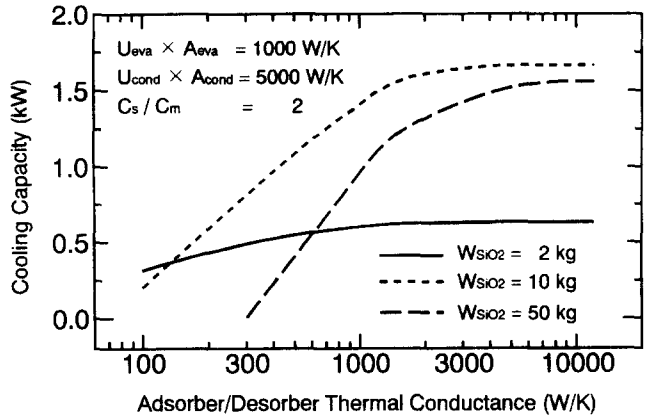

Fig. 4. (a) The effect of adsorber/desorber thermal conductance on cooling capacity.

Thermal capacitance ratio—The effects of silica-gel mass on cooling capacity, power density, COP, and chiller efficiency η were analyzed considering different adsorbent-to-metal thermal capacitance ratios ($C_{ps}/C_{p\ metal}$), namely, 0.5, 2 and 10. The values in each of the three lines in Fig. 3(a)–(d) were obtained by varying both the metal and adsorbent masses in the same proportion, so that the thermal capacitance ratio was kept constant for each plot. The plot for $C_{ps}/C_{p\ metal} = 10$ is included as an approximation to an ideal adsorber/desorber heat exchanger where the metal mass can be neglected in comparison with that of the adsorber.

Cooling capacity and power density become sensitive to the adsorbent-to-metal thermal capacitance ratio only for a relatively large amount of silica gel, as can be seen from Fig. 3(a) and (b). The power density is more sensitive to the adsorbent mass than to the thermal capacitance ratio.

The COP [Fig. 3(c)] and chiller efficiency η [Fig. 3(d)] values increase with higher adsorbent-to-metal thermal capacitance ratios. This result is due to the fact that reduction of the thermal capacitance of the adsorber/desorber heat exchangers causes low heat-input requirements. Thus, sensible heat losses can be minimized by using light-weight adsorber/desorber heat exchangers.

Adsorber/desorber thermal conductance

Figure 4(a)–(d) show results obtained by varying the adsorber/desorber thermal conductance, with the adsorbent-to-metal thermal capacitance ratio kept constant at 2 for three different adsorbent masses, namely, 2, 10 and 50 kg. Cooling capacity [Fig. 4(a)] increases with silica-gel mass from 2 to 10 kg and then decreases for 50 kg of silica-gel for the conditions under study because the external parameters (heat transfer, fluid-flow rates and refrigerant-flow rates) for 10 kg of silica-gel are taken as standard parameters (as is shown in Table 2) in our investigation. The power density [Fig. 4(b)] increases with decreasing adsorbent mass because it is defined by the cooling capacity per kg of SiO_2; COP [Fig. 4(c)]

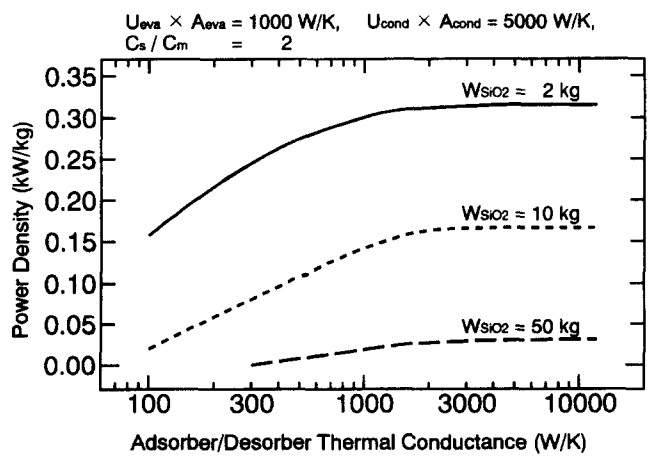

Fig. 4. (b) The effect of adsorber/desorber thermal conductance on power density.

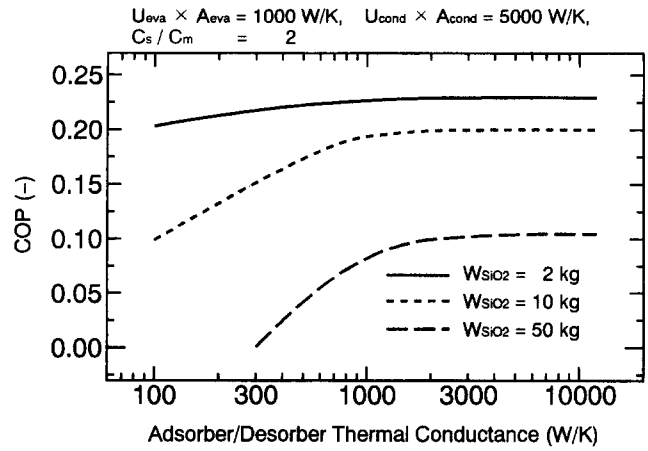

Fig. 4. (c) The effect of adsorber/desorber thermal conductance on COP.

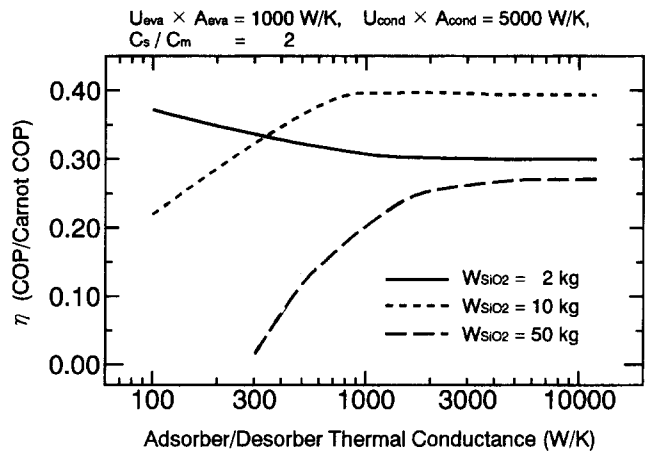

Fig. 4. (d) The effect of adsorber/desorber thermal conductance on chiller efficiency η.

Table 2. Standard conditions; cycle time = 330 s.

Hot water in:		Cooling water in:		Chilled water in:	
Temp (°C)	Flow (kg/s)	Temp (°C)	Flow (Ads + Cond) (kg/s)	Temp (°C)	Flow (kg/s)
50	0.58	30	0.91 (0.58 + 0.33)	12	0.06
Ads-Des cycle 300 s			Heat exchange cycle 30 s		

also increases with decreasing adsorbent mass. This last result may be attributed to the fact that smaller adsorbent masses mean reduced need for the heat input and, therefore, the COP improvement is observed. The chiller efficiency η [Fig. 4(d)] increases from 0.21 to 0.4 when the adsorber/desorber thermal conductance is increased from 100 to 1000W/K with 10 kg of silica-gel. With 50 kg of silica-gel, η increases with the increasing adsorber/desorber thermal conductance in the range between 300 and 3000W/K. For larger values, the η improvement is only marginal as is indicated by the fact that increasing the thermal conductance is no longer beneficial beyond 1000 and 3000W/K for 10 and 50 kg of silica-gel, respectively. The opposite tendency is observed with 2 kg of silica gel, η decreases when the adsorber/desorber thermal conductance is increased from 100 to 600W/K. With increasing thermal conductance, the COP improves slightly but the ideal COP (Carnot COP) improves significantly, which results in decreased chiller efficiency (η = COP/Carnot COP).

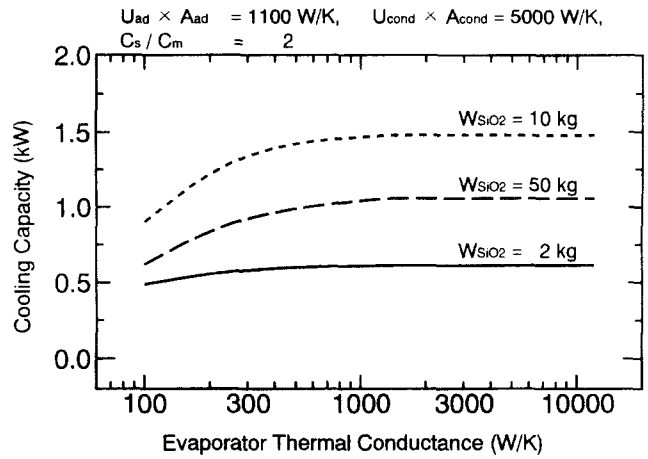

Fig. 5. (a) The effect of evaporator thermal conductance on cooling capacity.

Evaporator thermal conductance

Figures 5(a(–(d) show the effects of varying evaporator thermal conductance on cooling capacity, power density, COP, and chiller efficiency η, respectively. Qualitatively, the effect of evaporator thermal conductance is analogous to that of adsorber/desorber thermal conductance, since the trends of cooling capacity, power density, COP, and chiller efficiency η shown in Figs. 5(a)–(d) are similar to those

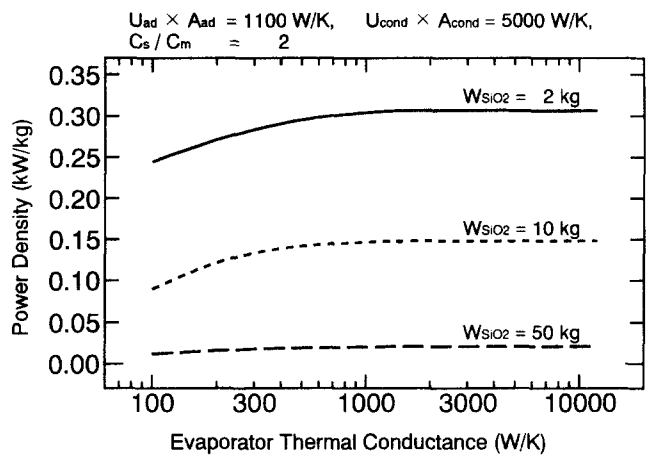

Fig. 5. (b) The effect of evaporator thermal conductance on power density.

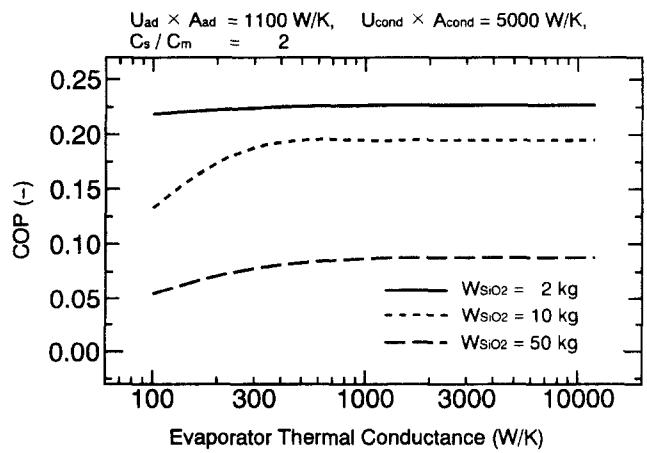

Fig. 5. (c) The effect of evaporator thermal conductance on COP.

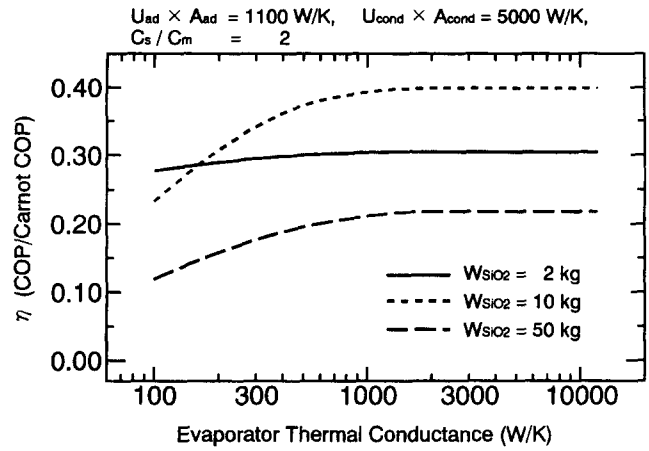

Fig. 5. (d) The effect of evaporator thermal conductance on chiller efficiency η.

discussed for Fig. 4(a)–(d), respectively. One interesting finding is that the evaporator thermal conductance of about 700W/K yields optimal system performance for both 10 and 50 kg of adsorbent mass. Improvement of evaporator thermal conductance beyond 300W/K is no longer beneficial for 2 kg of silica-gel mass. This observation is attributed to the fact that the water vapor pressure increases with increasing thermal conductance in the evaporator. The vapor is then more strongly adsorbed which results in a longer sensible heat-exchange-cycle requirement.

CONCLUSIONS

(i) Our model is most sensitive to adsorber/desorber thermal conductances, followed by the thermal conductance of the evaporator. (ii) The overall performance of the chiller can be improved by increasing the thermal capacitance ratios of the adsorbent masses to metal masses contained in each adsorber/desorber. (iii) Increasing the adsorbent masses (up to 12 kg of silica gel) in the adsorber/desorber heat exchanger is of benefit for both cooling capacity and chiller efficiency η. However, the power density and COPs decreased with increasing absorbent mass in the adsorber/desorber heat exchangers. (iv) The results of this study can be used to optimize the next generation of adsorption chiller designs. (v) Further investigations are needed on the effects of duration of adsorption–desorption cycle time and sensible heat-exchange cycle time in relation to operating temperatures and thermal conductances of the adsorber/desorber and evaporator.

Acknowledgements—We thank E. C. Boelman for technical support. Thanks are also due to our colleague R. Leutz for critical reading of the manuscript.

REFERENCES

1. Saha, B. B., Boelman, E. C. and Kashiwagi, T., *Energy—The International Journal*, 1995, **20**, 983.
2. Shelton, S. V., Wepfer, J. W. and Miles, D. J., *Heat Recovery Systems & CHP*, 1989, **9**, 233.
3. Härkönen, M. and Aittomäke, A., *Heat Recovery Systems & CHP*, 1992, **12**, 73.
4. Meunier, F., *Journal of Heat Recovery Systems*, 1985, **5**, 133.
5. Douss, N. and Meunier, F., *Chemical Engineering Science*, 1989, **44**, 225.
6. Sakoda, A. and Suzuki, M., *Journal of Chemical Engineering of Japan*, 1984, **17**, 52.
7. Saha, B. B. Boelman, E. C. and Kashiwagi, T., *ASHRAE Transactions*, 1995, **101**, Part 2, 348.
8. Ahern, J. E., *The Exergy Method of Energy Systems Analysis*, Wiley Interscience, NY, 1980.

NOMENCLATURE

A = Heat-transfer area (length^2)
C_p = Isobaric specific heat (energy/mass-deg)
D_s = Surface diffusivity (length^2/time)
D_{so} = Pre-exponential constant in Eq. (2) (length^2/time)
E_a = Activation energy for surface diffusion (energy/molecular mass)

$ksap$ = Overall mass-transfer coefficient (time^{-1})
m = Flow rate (mass/time)
$P_s(T)$ = Saturated vapor pressure at the temperature T(Pa) (force/length^2)
q = Amount adsorbed (mass/mass)
q^* = Equilibrium amount adsorbed (mass/mass)
Q_{chill} = Cooling capacity (energy)
Q_{hot} = Driving heat (energy)
R_p = Average radius of a particle (length)
T = Temperature (deg)
t = Time (sec)
U = Heat-transfer coefficient (energy/time-length^2-deg)
W = Weight (mass)

Subscripts

ad = Adsorber/desorber bed of silica gel
ads = Adsorption
Al = Aluminum
$chill$ = Chilled water
$cond$ = Condenser
Cu = Copper
des = Desorption
eva = Evaporator
$fHex$ = Fin (aluminum)
hot = Hot water
in = Inlet
$kHex$ = Heat-transfer tube (copper)
out = Outlet
s = Adsorbent (silica gel)
w = Refrigerant (distilled water)